

Fractionated Crystallization and Self-Nucleation Behavior of Poly(ethylene oxide) in Its Miscible Blends with Poly(3-hydroxybutyrate)

Pengju Pan, Li Zhao, Bo Zhu, Yong He, Yoshio Inoue

Department of Biomolecular Engineering, Tokyo Institute of Technology, 4259-B-55 Nagatsuta, Midori-ku 226-8501, Yokohama, Japan

Received 2 October 2009; accepted 11 February 2010

DOI 10.1002/app.32255

Published online 27 April 2010 in Wiley InterScience (www.interscience.wiley.com).

ABSTRACT: The fractionated crystallization and self-nucleation behavior of poly(ethylene oxide) (PEO) component in the miscible PEO/poly(3-hydroxybutyrate) (PHB) binary blends were investigated using differential scanning calorimetry (DSC) and small-angle X-ray diffraction (SAXS) under different crystallization conditions. The distribution of PEO component in the PEO/PHB blend greatly influences its fractionated crystallization behavior. The active heterogeneities, on which the semi-crystalline components in the molten state can nucleate at a small supercooling, are favored to locate out of the interlamellar regions of PHB crystals during the crystallization of PHB component. The PEO component confined in the interlamellar regions of PHB crystals crystallizes at an extremely large supercooling, which is induced by the homogeneous nucleation or less active heterogeneities,

while the PEO component expelled out of the interlamellar regions of PHB crystals can crystallize at a small supercooling due to the nucleation induced by active heterogeneities. In addition, the self-nucleation behavior of PEO component in the PEO/PHB blend is also affected by the active heterogeneities and the distribution of PEO phase in the blend. Different from the block copolymer systems, the PEO component confined into the interlamellar regions of PHB crystals can not be self-nucleated in the PEO/PHB blend without a nucleating agent (NA). © 2010 Wiley Periodicals, Inc. *J Appl Polym Sci* 117: 3013–3022, 2010

Key words: poly(ethylene oxide); poly(3-hydroxybutyrate); fractionated crystallization; self-nucleation; interlamellar region

INTRODUCTION

Poly(hydroxyalkanoate)s (PHAs), e.g., poly(3-hydroxybutyrate) (PHB), are biologically produced thermoplastics that have been drawing considerable attention as potential substitutes to the conventionally petrochemical plastics.^{1,2} Although PHB is one of the well-studied bacterial polyesters in the family of PHAs, it has a few serious drawbacks. For example, PHB is brittle because of the high crystallinity and large spherulite size, and it is also thermally unstable in the melt processing because its melting point is very close to the thermal degradation temperature.¹ These problems have been the major bottle-necks for its large-scale commercial applications. Polymer blending is a means widely used to modify the mechanical properties and processability of polymeric materials. For example, with the incorporation of poly(ethylene oxide) (PEO) or poly(ethylene glycol) (PEG) component, the toughness, flexibility, and elongation-at-break of poly(L-lactide) (PLLA) materi-

als have been modified significantly.^{3–6} Previous studies have reported that PHB (or its bacterial copolyesters) is miscible with the low-molecular-weight PEO or PEG in the molten state over whole blend compositions,^{7–12} while partially miscible or compatible with the high-molecular-weight PEO.^{13,14} PEO or PEG could be a potential plasticizer for PHB to improve its toughness and elongation-at-break.¹⁵ Besides, PEO (or PEG) possesses a much lower melting point ($T_m = 10–50^\circ\text{C}$, depending on molecular weight) than PHB ($T_m = \sim 180^\circ\text{C}$). Therefore, blending with PEO (or PEG) can decrease the melt-processing temperature of PHB and thus lessen its thermal decomposition.

In the crystallization process from a molten state, the polymers usually nucleate on the existing heterogeneities (e.g., catalyst debris, impurities, and other types of heterogeneities of unknown nature) at a relatively smaller supercooling. However, if a semicrystalline polymer is finely dispersed in an immiscible matrix as isolated domains where the active heterogeneities is scarce, the crystallization in these domains can only proceed via a homogeneous nucleation at a large supercooling. When such a dispersed system is cooled from the melt, a series of crystallization exotherms are usually observed and a fractionated

Correspondence to: Y. Inoue (inoue.y.af@m.titech.ac.jp).

crystallization phenomenon occurs.¹⁶ The fractionated and confined crystallization has been found in a variety of immiscible polymer blends^{17–19} and block copolymers,^{20–25} which consist of a blend/block component crystallizing in more than one step at different supercoolings.

Compared with the amorphous/amorphous or amorphous/crystalline polymer blends, the binary crystalline/crystalline blends have received much less attention. However, the crystallization behavior of the crystalline/crystalline polymer blends is of great interest, because the crystalline morphology and crystallization kinetics of the blend components can be manipulated by a variety of variables.^{26–28} In our previous studies,^{29,30} it was first found that the fractionated and confined crystallization also takes place in the crystalline/crystalline miscible polymer blends, e.g., PEO/poly(butylene succinate) (PBS) blend, which is somewhat analogous to that of the immiscible binary blends or block copolymers. Here, the two crystalline components were referred to as A and B, where A possesses a lower bulk crystallization temperature (T_c) and a lower melting temperature (T_m) than B. The lack of enough active heterogeneities, which can induce the heterogeneous nucleation of polymer, in the confined regions of the B crystal lamellae results in the fractionated crystallization of the component A.

However, the fractionated crystallization behavior of a crystalline/crystalline miscible polymer blend should be different from that of an immiscible blend or block copolymer. For a binary miscible blend system, during the crystallization of the component B, the component A will be able to reside in the interlamellar, interfibrillar, or interspherulitic regions with the domain size ranging from several nanometers to micrometers.³¹ The smaller size of the confined region, the more lack of active heterogeneities is.¹⁴ Therefore, the phase segregation and redistribution of the component A after the crystallization of the component B will greatly influence the fractionated crystallization behavior of the component A.

Fillon et al.³² have reported that the self-nuclei can be generated and studied in a controlled fashion by use of a suitable self-nucleation protocol in the DSC analysis. This approach has been widely employed to study the self-nucleation^{33–37} and fractionated crystallization^{23–25} of polymers. They divided the self-nucleation temperature (T_s) in three domains.³² In domain I, the complete melting is attained and no memory effect of the prior crystallization exists, which generally takes place when T_s is located above the upper foot of the melting endotherm. Domain II or self-nucleation domain locates at lower T_s region. The T_s temperatures of domain II are high enough to melt almost all crystals in the sample, but small fragments or seeds that can act as self-nucleating

nuclei remain and the nucleation density can be enormously increased by a small change in T_s . In domain III, the sample is partially molten, resulting in the self-nucleation and annealing of unmelted crystals. By examining the fractionated crystallization of several di- and tri-block copolymers, Muller et al.^{23,34} have found that the crystals induced by homogeneous nucleation at very low temperatures cannot be nucleated by the self-nucleating nuclei in domain II. Moreover, the domain III splits into a pure annealing domain as well as a self-nucleation and annealing domain at lower T_s region. This phenomenon is distinct from that found in the classical self-nucleated crystallization of polymers.

As for the miscible blend system of two crystalline components A and B, after the crystallization of high- T_c B component and prior to the crystallization of low- T_c A component, the amorphous A component mixes with the amorphous phase of the B component in the confined interlamellar regions or out of the interlamellar regions of the B crystalline lamellae. Therefore, the self-nucleation behavior in the crystalline/crystalline miscible polymer blend could be more complex and much different from those occurred in the homopolymers or block copolymers. On the other hand, aside from the PEO/PBS blend system,^{29,30} the fractionated crystallization of the PEO component has also been observed in the PEO/PHB miscible blends.³⁸ However, the effects of crystallization conditions of PHB and the distribution of PEO on the fractionated and confined crystallization of the PEO component have been unexplored. Since the self-nucleation method has been widely employed to study the fractionated crystallization of block copolymers, it may be valuable to extend this method to the crystalline/crystalline miscible blend systems.

As described above, many studies on the fractionated and confined crystallization of the immiscible polymer blend systems^{17–19} and block copolymers^{20–25} have been conducted; however, very few studies were focused on the crystalline/crystalline miscible polymer blend systems.^{29,30} This work is aiming to investigate the fractionated crystallization and self-nucleation behavior of the one crystalline component that was confined in the crystalline lamellae of the other component in their binary miscible blends. In this article, the fractionated crystallization behavior of the PEO component in the miscible PEO/PHB blends under the different conditions, that is, the untreated PEO/PHB blend, the PEO/PHB blend containing a nucleating agent (NA), and the PEO/PHB blend thermally treated to induce the self-nucleation of PHB component, was investigated and compared by differential scanning calorimetry (DSC) and small-angle X-ray diffraction (SAXS) techniques. The effects of NA and phase segregation of the PEO

component on the fractionated and confined crystallization of the crystalline/crystalline polymer blends were studied. Furthermore, the self-nucleation behavior of the PEO component in the miscible PEO/PHB blends was investigated.

EXPERIMENTAL

Materials

PEO ($M_v = 2.0 \times 10^4$ g/mol) was purchased from Nacalai Tesque and used without further purification. PHB ($M_w = 1.9 \times 10^5$ g/mol, $M_w/M_n = 2.35$) was purchased from Aldrich Chemical Co. (USA), and it was purified by precipitation in ethanol from a chloroform solution. Saccharin, a typical NA of PHB,³⁹ was purchased from Kanto Chemical Co. (Japan). The particle size of saccharin is about 3 μm , which was determined by a polarized optical microscopy (POM) analysis.

Preparation of blend samples

The PEO/PHB blends were prepared by a solution cast method using chloroform as a common solvent. Both polymers were dissolved and mixed in chloroform with the desired weight proportions (total polymer concentration was ~ 1 g/50 mL). The blends containing 2 wt % saccharin were prepared by adding the methanol solution of saccharin to the chloroform solution of PEO/PHB blends. The solution was well-stirred and subsequently cast on a Petri dish, and the solvent was allowed to evaporate under an ambient condition. Since the methanol solvent may influence the crystallization of PEO,⁴⁰ all films obtained were placed in an oven at $\sim 25^\circ\text{C}$ under vacuum for 1 week to eliminate the residual solvent. To prepare the film samples for various measurements, the samples were subsequently hot-pressed after melting at 190°C for 2 min, followed by a quenching to $\sim 25^\circ\text{C}$ under an ambient condition. The resulting samples were kept under vacuum at $\sim 25^\circ\text{C}$ for 2 months before the various analyses. The blends are denoted as PEO x /PHB y , where x and y represent the weight percentages of PEO and PHB, respectively. The description for the blend samples is shown in Table I.

TABLE I
Description for Blend Samples

PEO/PHB-UT	untreated PEO/PHB blend
PEO/PHB-NA	PEO/PHB blend containing 2 wt % saccharin as a nucleating agent
PEO/PHB-SN _{PHB}	PEO/PHB blend with self-nucleation treatment of PHB component

UT, untreated; NA, nucleating agent; SN, self-nucleation.

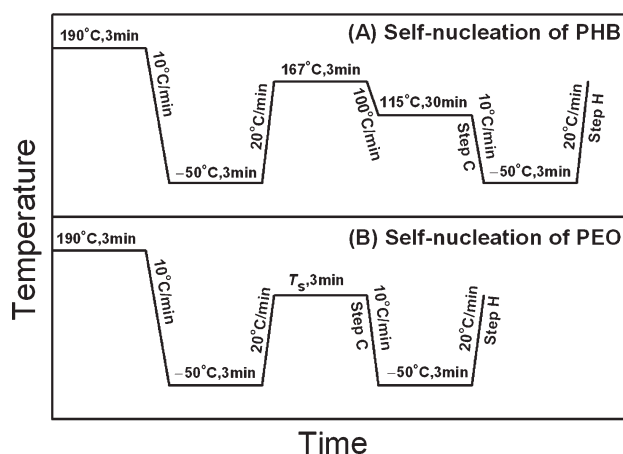


Figure 1 DSC thermal programs for (A) the self-nucleation treatment of PHB component in the PEO/PHB-SN_{PHB} sample and (B) the self-nucleated crystallization of PEO component in the PEO/PHB blends. Steps C and H are the cooling and heating scans, respectively.

Differential scanning calorimetry

DSC measurements were performed on a Pyris Diamond DSC (Perkin-Elmer Japan Co., Tokyo, Japan) equipped with an intracooler 2P cooling accessory. The temperature and heat flow at different heating rates were calibrated by use of an indium standard. The samples (~ 7 mg) were weighed and sealed in an aluminum pan. To study the nonisothermal crystallization, the PEO/PHB-UT, PEO/PHB-NA, and neat PEO samples were first melted at 190°C for 3 min to erase the thermal history, and then cooled to -50°C at a cooling rate of $10^\circ\text{C}/\text{min}$, followed by reheating to 190°C at a scanning rate of $20^\circ\text{C}/\text{min}$ to observe the melting behavior. In the DSC analysis, the temperatures corresponding to the peak tops of the crystallization exotherms and melting endotherms were taken as the crystallization temperature (T_c) and melting temperature (T_m), respectively.

The self-nucleation procedures used in this work are illustrated in Figure 1. As concerning the PEO/PHB-SN_{PHB} sample, the PHB component was treated by a self-nucleated crystallization. The self-nucleation temperature (T_s) was selected as 167°C [Fig. 1(A)], since all of the PHB crystals in the PEO/PHB blend disappeared at this temperature, as observed by POM. For the self-nucleation treatment of PEO component, different T_s values ranging over 46 – 100°C were chosen [Fig. 1(B)], and these T_s values are much lower than the T_m value of PHB component (173°C for the neat PHB used in this study).

Small-angle X-ray scattering

SAXS measurements were performed on a Rigaku RU-200 system (Rigaku Co., Tokyo, Japan) worked at 40 kV and 200 mA under room temperature. Nickel-filtered Cu K α radiation ($\lambda = 0.154$ nm) was

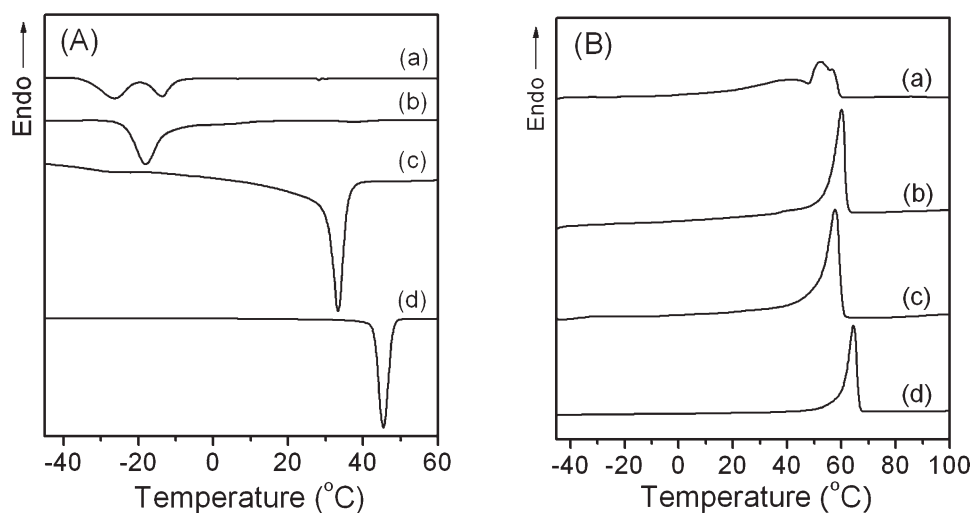


Figure 2 DSC curves recorded in (A) the cooling scans at 10°C/min and (B) the subsequent heating scans at 20°C/min for (a) PEO20/PHB80-UT, (b) PEO20/PHB80-NA, (c) PEO20/PHB80-SN_{PHB}, and (d) neat PEO samples. The heat flows of the blend samples were enlarged eight times.

used. SAXS profiles were recorded in the 2θ range of 0.1° – 3° . Each step increased 2θ by 0.004° , and X-ray was collected for 15 s at each step. The thermal procedures of blend samples for SAXS analysis are the same to the ones used in the nonisothermal crystallization process.

RESULTS AND DISCUSSION

Fractionated crystallization of PEO in PEO/PHB blend

In the case of PEO/PBS blends, the fractionated crystallization of PEO component is only observed at low PEO content (not more than 30 wt %).²⁹ Avella et al.³⁸ have reported that the fractionated crystallization of PEO component can only be clearly detected during the fast cooling process of the PEO/PHB blends when the PEO content is around 20 wt %. Therefore, two blend compositions, that is, PEO20/PHB80 and PEO30/PHB70, were selected to study the fractionated crystallization behavior of PEO/PHB blends in this work. Figure 2 shows the DSC curves recorded in the cooling and subsequent heating scans for neat PEO and the three different PEO20/PHB80 blend samples, that is, (a) the untreated PEO20/PHB80 sample (PEO20/PHB80-UT), (b) the PEO20/PHB80 sample containing 2 wt % saccharin as a NA (PEO20/PHB80-NA), and (c) the PEO20/PHB80 sample thermally treated by the self-nucleated isothermal crystallization of PHB component at 115°C according to the thermal program shown in Figure 1(A) (PEO20/PHB80-SN_{PHB}). The DSC cooling scans were conducted from 190 to -50°C at a cooling rate of 10°C/min for the PEO20/PHB80-UT and PEO20/PHB80-NA samples, whereas

from 115 to -50°C for the PEO20/PHB80-SN_{PHB} sample. For clarity, only the temperature ranges corresponding to the crystallization and melting of PEO component were depicted in Figure 2.

As seen in Figure 2(A), the DSC cooling curve of neat PEO exhibits a single sharp crystallization peak at $\sim 45^\circ\text{C}$, corresponding to the crystallization of bulk PEO induced by heterogeneous nucleation.^{23,29,38} In the case of the PEO20/PHB80-UT sample [curve (a)], two major crystallization exotherms, locating at -13 and -27°C , can be detected upon cooling. Analogous to the PEO/PBS blends with PEO content not more than 20 wt %, ²⁹ when PEO is the minor component in the PEO/PHB miscible blends, most of the PEO component resides in the interlamellar regions of PHB crystals.¹⁴ Since the T_g of PEO is around -50°C , the PEO component in the PEO20/PHB80-UT sample undergoes an extremely large supercooling before crystallization, which is a characteristic of the homogeneously nucleated crystallization.²³ The interlamellar distance is fairly smaller than the size of active heterogeneities, and the number of amorphous layers in the interlamellar regions is much larger than that of the available active heterogeneities. Therefore, in this case, the crystallization of PEO component is predominantly induced by the homogeneous nucleation or much less active heterogeneities at an extreme large supercooling. This finding coincides with that observed in the PEO/PBS miscible blends with a low PEO content.²⁹

For the PEO20/PHB80-NA sample, only a major crystallization peak of PEO component is detected at -18°C , as shown in curve (b) of Figure 2(A). This is distinct from that reported previously by Avella et al.³⁸ They have reported that the NA, saccharin, can considerably induce the heterogeneous nucle-

ation of PEO in the PEO/PHB blends. Most of the PEO component in the PEO40/PHB60 blend sample containing 2 wt % saccharin could crystallize at a small supercooling, similar to the crystallization of neat PEO. This may be attributable to the different distribution of PEO component in the blend that depends on the blend composition. According to our previous results,^{29,30} in the PEO40/PHB60 blend, most of the PEO component is likely to be excluded from the interlamellar regions of PHB crystals, whereas most of the PEO component in the PEO20/PHB80 blend is incorporated in the interlamellar regions of PHB crystals. These results suggest that the PEO component confined in the interlamellar regions of PHB crystals is free from the active heterogeneous nucleation, even in the blend samples containing a NA. A possible explanation is that most of the saccharin molecules aggregate into particles with the micrometer scale, whose size is much larger than the interlamellar spacings of PHB crystals (about several nanometers). Therefore, for the PEO component confined between the interlamellar regions of PHB crystals, saccharin has little heterogeneous nucleation effect on its crystallization.

With regard to the PEO20/PHB80-SN_{PHB} sample, two crystallization peaks of the PEO component can be detected in the cooling process [curve (c) of Fig. 2(A)], that is, a major exotherm at 33°C and a broad and weak exotherm at -27°C. In the self-nucleated crystallization of PHB [Fig. 1(A)], the premelting at $T_s = 167^\circ\text{C}$ allows the crystallization of PHB component to be nucleated by the tremendous unmelted crystal fragments, and the annealing at 115°C for 30 min is enough for the crystallization of PHB component. Because of the slow growth rate of the PHB crystals and high diffusion rate of the PEO component at 115°C, most of the PEO component could be expelled out of the interlamellar regions of PHB crystals. It seems that there are enough active heterogeneities out of the interlamellar region of PHB crystals, which can induce the crystallization of PEO at a very small supercooling. It is noteworthy that there is still some PEO confined in the interlamellar regions of PHB crystals, which crystallizes at a large supercooling similar to the PEO component in the PEO20/PHB80-UT sample.

After the nonisothermal crystallization process, the melting behavior of three kinds of PEO20/PHB80 blend samples was investigated by DSC analysis. As shown in Figure 2(B), neat PEO exhibits a single melting peak at around 64°C. The T_m values of PEO component in the PEO/PHB blends slightly decrease, compared with neat PEO. The depression in T_m values has been widely observed in the crystalline/crystalline or crystalline/amorphous polymer blends. The T_m values and the shapes of the melting endotherms for the PEO component in the PEO20/

PHB80-NA and PEO20/PHB80-SN_{PHB} samples are almost the same. Usually, for the same crystalline component, the melting behavior is dominated by the lamellar thickness and perfection of the crystal. The similar melting behavior of the PEO20/PHB80-NA and PEO20/PHB80-SN_{PHB} samples might suggest the similar lamellar thickness and the perfection of the PEO crystals formed in both samples.

It should be noted that the melting peak of PEO component in the PEO20/PHB80-UT sample is broader than that in the other samples. Three peaks, situated at 39, 52, and 57°C, can be detected in the melting region of the PEO20/PHB80-UT sample. The multiple fractionated crystallization of PEO component in the PEO20/PHB80-UT sample, corresponding to the crystallization peaks at -13 and -27°C [curve (a) in Fig. 2(A)], could be responsible for this multiple and complex melting behavior. The lowest melting peak observed at 39°C should be ascribed to the melting of PEO crystals that are crystallized at the largest supercooling and induced by the homogeneous nucleation.

In Figure 3 are compared the crystallization and subsequent melting behavior of the PEO component in the three kinds of PEO30/PHB70 blend samples. As concerning the thermally untreated PEO30/PHB70 sample (PEO30/PHB70-UT), three broad crystallization peaks (located at -24, 21, and 37°C) corresponding to the fractionated crystallization of PEO component are detected, which is similar to the PEO/PBS blend containing 30 wt % PEO.²⁹ The PEO component expelled out of the interlamellar regions of PHB crystals crystallizes at a small supercooling by the heterogeneous nucleation, whereas the crystallization of PEO confined in the interlamellar regions is mainly induced by the less active heterogeneities or homogenous crystallization at a high supercooling. From the magnitudes of these crystallization peaks, it can be estimated that the fraction of PEO incorporated in the interlamellar regions of PHB crystals is comparable to that expelled out of the interlamellar regions.

With the addition of 2 wt % saccharin as a NA, the crystallization temperatures of PEO in the PEO30/PHB70 sample (PEO30/PHB70-NA) shift to new regions with peak tops at -15, 6, and 40°C [curve (b) of Fig. 3(A)]. The magnitude of crystallization peak at 37°C for the PEO30/PHB70-UT sample is nearly equal to the peak at 40°C for the PEO30/PHB70-NA sample. The crystallization of PEO at 37°C for the PEO30/PHB70-UT sample is ascribed to the PEO component distributed out of the interlamellar regions of PHB crystals. Because of the heterogeneous nucleation effect, the crystallization temperature of the PEO component residing outside the interlamellar regions of PHB crystals in the PEO30/PHB70 blend shifts from 37 to 40°C, with the

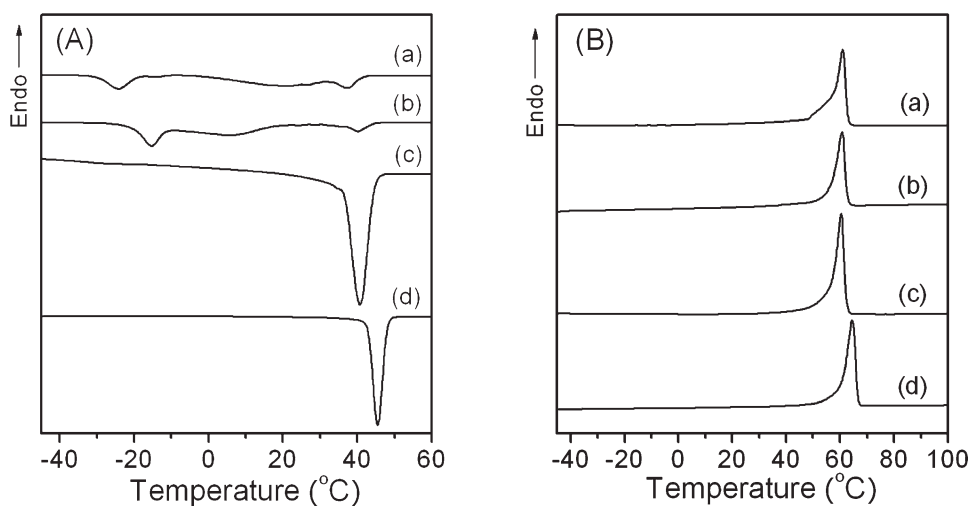


Figure 3 DSC curves recorded in (A) the cooling scans and (B) subsequent heating scans for (a) PEO30/PHB70-UT, (b) PEO30/PHB70-NA, (c) PEO30/PHB70-SN_{PHB}, and (d) neat PEO samples. The heat flows of the blend samples were enlarged five times.

incorporation of 2 wt % saccharin. For the PEO30/PHB70 sample thermally treated to induce the self-nucleation of PHB component (PEO30/PHB70-SN_{PHB}), a major sharp crystallization peak of PEO at 40°C is observed [curve (c) in Fig. 3(A)], which is similar to the DSC curve of the PEO20/PHB80-SN_{PHB} sample. As seen in Figure 3(B), the melting curve [curve (a)] of the PEO30/PHB70-UT sample exhibits a shoulder peak prior to the major melting peak, ascribing to the fractionated crystallization of PEO component.

Analogous to the immiscible blends or block copolymers,¹⁶ the fractionated and confined crystallization of PEO component in the miscible PEO/PHB blends with a low PEO content is due to the lack of active heterogeneities within the interlamellar regions of PHB crystals.²⁹ However, when the PEO component is expelled from the interlamellar regions of PHB crystals, most of PEO can crystallize at a low supercooling induced by the active heterogeneities. The addition of NA, i.e., saccharin, affects little on the crystallization of PEO component confined in the interlamellar regions of PHB crystals, because the NA particles cannot enter into these confined regions. It is reasonable to conclude that the distribution of active heterogeneities in the miscible PEO/PHB blends after the crystallization of PHB component is restricted by the size of the confined regions. The active heterogeneities are favored to reside in the interfibrillar or interspherulitic regions of PHB spherulites with larger size. Because of the nonuniform distribution of the active heterogeneities, the redistribution of PEO component during the crystallization of PHB component greatly influences the fractionated and confined crystallization behavior of the PEO component.

SAXS analysis

The microstructures of PEO/PHB blends were further analyzed by SAXS measurements. Figure 4 shows the Lorentz-corrected SAXS profiles for the PEO20/PHB80 and PEO30/PHB70 blends with different crystallization conditions. The scattering vector q was calculated from the equation $q = 4\pi\sin(\theta/\lambda)$, where 2θ is the scattering angle and λ represents the wavelength of X-ray. The SAXS profiles of neat PEO

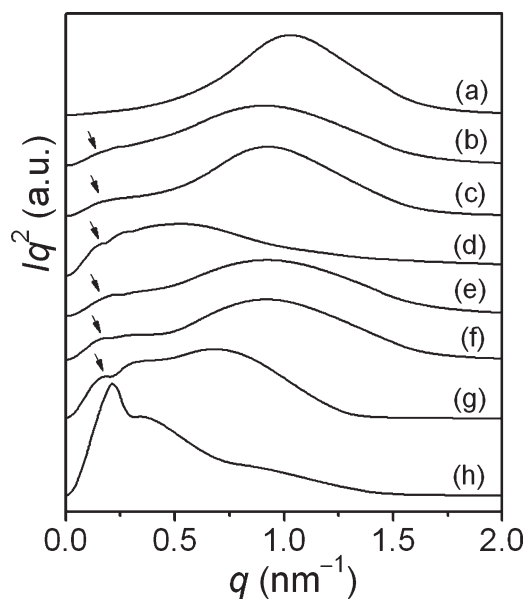


Figure 4 Lorentz-corrected SAXS profiles of (a) neat PHB, (b) PEO20/PHB80-UT, (c) PEO20/PHB80-NA, (d) PEO20/PHB80-SN_{PHB}, (e) PEO30/PHB70-UT, (f) PEO30/PHB70-NA, (g) PEO30/PHB70-SN_{PHB}, and (h) neat PEO. The curves were normalized and shifted vertically for clarity. The arrows indicate the scattering peaks of PEO component.

and PHB are also shown in Figure 4 for comparison. The profile shape and position of the scattering peaks for PEO20/PHB80-UT or PEO30/PHB70-UT sample are similar to those of the corresponding PEO/PHB sample containing 2 wt % saccharin, which likely indicates that the addition of saccharin affects little on the microstructure of the PEO/PHB blends. The long period (LP) can be calculated using the equation $LP = 2\pi/q_{\max}$, where q_{\max} is the maximum q value in the Lorentz-corrected SAXS plot (Fig. 4). The lower the q_{\max} value, the higher the LP value is. As seen in curves (d) and (g) of Figure 4, the scattering peak of PHB significantly shifts to the low- q side, after the self-nucleation treatment of PHB component in both the PEO20/PHB80 and PEO30/PHB70 samples. It can be concluded that the LP value of PHB crystals increases considerably with the self-nucleated crystallization at 115°C. As discussed above, the self-nucleation treatment allows for the fast crystallization of PHB component at high temperature (i.e., 115°C) on the tremendous unmelted crystal fragments, accounting for the larger lamellar thickness and higher perfection of the PHB crystals.

As seen in Figure 4, a scattering shoulder (marked by an arrow) at the low- q range beside the main scattering peak is identified for the PEO/PHB blend samples. The position of these shoulders is almost the same to that of the main scattering peak of neat PEO, suggesting that the scattering shoulder corresponds to the scattering of the lamellar stack of PEO component. Since all the blend samples were aged at $\sim 25^\circ\text{C}$ for 2 months before the measurements, the prolonged aging can induce the crystallization of some amount of PEO component in the blend system.¹⁴ The magnitude of the scattering shoulder increases with the PEO composition. Compared with the PEO/PHB-UT and PEO/PHB-NA samples, the magnitude of the PEO scattering shoulder is larger for the PEO/PHB-SN_{PHB} sample. This is in agreement with the DSC results, and further indicates that the PEO component is expelled out of the interlamellar regions of PHB crystals during the self-nucleated crystallization of PHB component, which facilitates the crystallization of PEO component during aging at $\sim 25^\circ\text{C}$.

Self-nucleation behavior of PEO in PEO/PHB blend

Apart from the incorporation of NA, a self-nucleation procedure is an alternative approach to import the effective nuclei to the semicrystalline polymer confined in the nanometer range.^{23–25,34} Typically, the heterogenous nucleation forms at preferential sites such as nucleating agent, impurity, or phase boundary. The self-nucleation was induced by the

residual nuclei, when the crystalline sample was melted at relatively low temperature and the previous crystal nuclei were not completely removed. Both the heterogenous and self-nucleation crystallizations occur at higher temperature and require less energy than homogeneous nucleation. The self-nucleation depends on the melting conditions prior to crystallization, and it disappears with an increase in the fusion temperature or time and cannot be observed when the thermal history of sample was completely removed at higher melting temperature. However, the heterogeneous nucleation is generally independent on the melting conditions.

Figure 5(A) shows the DSC curves recorded in the cooling process of the PEO20/PHB80-UT sample from the indicated self-nucleation temperature (T_s); the thermal procedure for the self-nucleation of PEO component is shown in Figure 1(B). Figure 5(B) depicts the DSC curves recorded in the subsequent heating process after the self-nucleation at the indicated temperatures. At $T_s = 100^\circ\text{C}$, the DSC cooling curve exhibits two major crystallization peaks, that is, the high- and low- T ones with the peak tops at 12 and -28°C , respectively. At $T_s = 65\text{--}100^\circ\text{C}$, no appreciable change is observed concerning the shape of DSC curves and the relative magnitudes of high- and low- T crystallization peaks (data not shown). At $T_s = 58\text{--}65^\circ\text{C}$, the area of the high- T crystallization peak decreases gradually with T_s . The high- T crystallization peak disappears at $T_s < 58^\circ\text{C}$. At $T_s = 58^\circ\text{C}$, the crystallization of PEO starts immediately from the beginning of the cooling run and a crystallization peak [marked by an arrow in Fig. 5(A)] is observed just below T_s , suggesting that the self-nucleation and annealing processes are simultaneously present.^{23,32,34} This can be confirmed in the subsequent DSC heating scan of the sample with the same T_s value of 58°C [Fig. 5(B)], where a peak shoulder locating at the high-temperature side ($\sim 60^\circ\text{C}$, marked by an arrow) of the melting peak can be observed. It can be concluded that the self-nucleation domain (or domain II) and domain III start at $T_s = 65$ and 58°C , respectively.

At $T_s < 58^\circ\text{C}$, a further decrease in T_s will induce an increase in the amount of unmelted crystals and the number of annealed crystals, as indicated by the increase in the magnitude of the higher melting temperature endotherm, which shifts to lower temperature as T_s is increased (see curves corresponding to the T_s temperatures of 56, 54, and 52°C). As shown in Figure 5(A), the trend in variation of the low- T crystallization peak with T_s is distinct from that of its high- T counterpart. At $T_s > 54^\circ\text{C}$, no discernible alteration in the shape and area of the low- T crystallization peak is detected with a decrease in the T_s value. At $T_s < 54^\circ\text{C}$, the low- T crystallization peak shifts toward the low-temperature side and its area

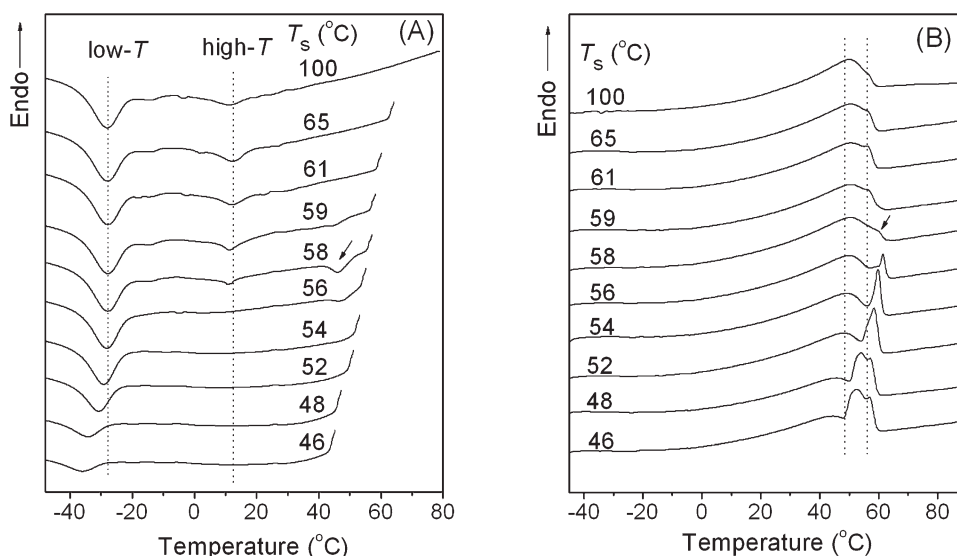


Figure 5 DSC curves recorded (A) upon cooling from the indicated T_s temperatures at a rate of $10^\circ\text{C}/\text{min}$ and (B) during the subsequent heating scans at $20^\circ\text{C}/\text{min}$ after the self-nucleation of PEO component at the indicated temperatures for the PEO20/PHB80-UT sample.

decreases with a decrease in T_s . At $T_s < 54^\circ\text{C}$, except for the low- T crystallization peak, no crystallization peak at higher temperature can be observed. These results suggest that the domain II process completely disappears at $T_s = 54^\circ\text{C}$, and moreover the domain III process differs from that observed in the classical self-nucleation behavior.^{32,34} Normally, the domain III includes both the self-nucleation and annealing processes,^{32,34} as indicated by the crystallization behavior of PEO component over the high- T crystallization region at $T_s < 58^\circ\text{C}$. However, over the low- T crystallization region, the domain III process only contains the annealing behavior. This likely suggests

that, in the PEO/PHB-UT sample, the PEO component confined in the interlamellar regions of PHB crystals, which crystallizes at low- T region, cannot be self-nucleated. This finding is different from that observed for the polymeric segments confined in the block copolymers, such as poly(styrene-*b*-ethylene-*b*-caprolactone),^{23,34} in which a part of polymeric blocks confined in the nanoscale domains can undergo the self-nucleated crystallization.

As discussed above, the low- T crystallization region around -30°C [Fig. 5(A)] corresponds to the crystallization of PEO component restricted in the interlamellar regions of PHB crystals; the crystalli-

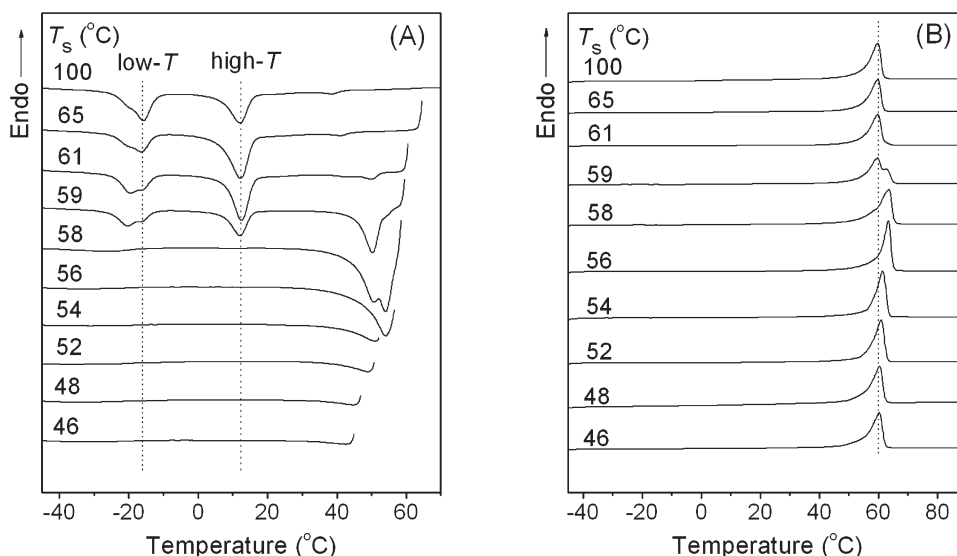


Figure 6 DSC curves recorded (A) upon cooling from the indicated T_s temperatures at a rate of $10^\circ\text{C}/\text{min}$ and (B) during the subsequent heating scans at $20^\circ\text{C}/\text{min}$ after the self-nucleation of PEO component at the indicated temperatures for the PEO20/PHB80-NA sample.

zation of this portion of PEO is mainly induced by the homogeneous nucleation or much less active heterogeneities at an extremely high supercooling. At such a high supercooling, it is difficult to expel the amorphous PHB molecules that are in the vitrification state at this temperature (the T_g of PHB is around -5°C) from the growth front of the PEO crystals in the crystallization process. Therefore, only the imperfect PEO crystals with thinner lamellae could be formed. Moreover, these resulting PEO crystals are confined among the amorphous PHB molecules in the interlamellar regions of PHB crystals. This nanoscale confinement might induce the PEO component free from the self-nucleated crystallization.

Figure 6 shows the DSC cooling curves from the indicated T_s temperatures and subsequent heating scan for the PEO component in the PEO20/PHB80 sample containing 2 wt % saccharin as a NA. At $T_s = 100^\circ\text{C}$, two major crystallization peaks, that is, a high- T exotherm at 12°C and a low- T one at -17°C , are detected upon cooling. As seen in Figure 6, the PEO crystals crystallized at both the high- and low- T crystallization regions exhibit the same classical nucleation domains; the self-nucleation domain (or domain II) starts at $T_s = 65^\circ\text{C}$ and the domain III containing both the self-nucleation and annealing processes starts at $T_s = 60^\circ\text{C}$.

Comparing the results shown in Figures 5 and 6, it can be concluded that the addition of NA influences the self-nucleation behavior of the PEO component in the PEO/PHB blends. For the PEO20/PHB80-NA sample, the PEO component confined into the interlamellar regions of PHB crystals undergoes the self-nucleated crystallization, which, however, is absent in the case of PEO20/PHB80-UT sample. It is considered that, over the low- T crystallization region, the crystallization of PEO component in PEO20/PHB80-NA sample is induced by the less active heterogeneities. The microstructure of the PEO crystals produced under these conditions could be analogous to that of the PEO crystals grown over the high- T crystallization region. Thus, these PEO crystals have the similar melting and self-nucleation behavior to those developed over the high- T crystallization region.

CONCLUSIONS

The fractionated crystallization and self-nucleation behavior of the PEO component in the miscible PEO/PHB blends under different crystallization conditions have been investigated by DSC and SAXS. The distribution of PEO component in the PEO/PHB blends after the crystallization of PHB component greatly influences the fractionated crystallization of the PEO component. The active heterogene-

ities are favored to locate out of the interlamellar regions of PHB crystals. The PEO component confined in the interlamellar regions of PHB crystals crystallizes at an extremely high supercooling induced by the homogeneous nucleation or less active heterogeneities, whereas the PEO component expelled out of the interlamellar regions of PHB crystals can crystallize at a low supercooling induced by the active heterogeneities. The self-nucleation behavior of PEO component in the PEO/PHB blends is affected by the heterogeneities (e.g., NA) and its distribution. For the PEO component expelled out of the interlamellar regions of PHB crystals, it shows the classical three domains depending on T_s . For the PEO component confined into the interlamellar regions of PHB crystals, the self-nucleated crystallization cannot be observed in the blends without NA.

References

- Pan, P.; Inoue, Y. *Prog Polym Sci* 2009, 34, 605.
- Lenz, R. W.; Marchessault, R. H. *Biomacromolecules* 2005, 6, 1.
- Nijenhuis, A. J.; Colstee, E.; Grijpma, D. W.; Pennings, A. J. *Polymer* 1996, 37, 5849.
- Hu, Y.; Rogunova, M.; Topolkaev, V.; Hiltner, A.; Baer, E. *Polymer* 2003, 44, 5701.
- Hu, Y.; Hu, Y. S.; Topolkaev, V.; Hiltner, A.; Baer, E. *Polymer* 2003, 44, 5711.
- Kulinski, Z.; Piorkowska, E. *Polymer* 2005, 46, 10290.
- Avella, M.; Martuscelli, E. *Polymer* 1988, 29, 1731.
- Park, S. H.; Lim, S. T.; Shin, T. K.; Choi, H. J.; Jhon, M. S. *Polymer* 2001, 42, 5737.
- Na, Y.-H.; He, Y.; Asakawa, N.; Yoshie, N.; Inoue, Y. *Macromolecules* 2002, 35, 727.
- You, J.-W.; Chiu, H.-J.; Don, T.-M. *Polymer* 2003, 44, 4355.
- Tan, S. M.; Ismail, J.; Kummerlowe, C.; Kammer, H. W. *J Appl Polym Sci* 2006, 101, 2776.
- Lim, J. S.; Noda, I.; Im, S. S. *J Polym Sci Part B: Polym Phys* 2006, 44, 2852.
- He, Y.; Asakawa, N.; Inoue, Y. *Polym Int* 2000, 49, 609.
- Zhao, L.; Kai, W.; He, Y.; Zhu, B.; Inoue, Y. *J Polym Sci Part B: Polym Phys* 2005, 43, 2665.
- Parra, D. F.; Fusaro, J.; Gaboardi, F.; Rosa, D. S. *Polym Degrad Stab* 2006, 91, 1954.
- Arnal, M. L.; Matos, M. E.; Morales, R. A.; Santana, O. O.; Muller, A. J. *Macromol Chem Phys* 1998, 199, 2275.
- Frensch, H.; Harnischfeger, P.; Jungnickel, B. J. In *Multiphase Polymers: Blends and Ionomers*; Utracky, L. A., Weiss, R. A., Eds.; ACS Symposium Series; American Chemical Society: Washington, DC, 1989; Vol. 395, p 101.
- Everaert, V.; Groeninckx, G.; Koch, M. H. J.; Reynaers, H. *Polymer* 2003, 44, 3491.
- Yordanov, C.; Minkova, L. *Eur Polym J* 2005, 41, 527.
- Zhu, L.; Huang, P.; Chen, W. Y.; Ge, Q.; Quirk, R. P.; Cheng, S. Z. D.; Thomas, E. L.; Lotz, B.; Hsiao, B. S.; Yeh, F.; Liu, L. *Macromolecules* 2002, 35, 3553.
- Opitz, R.; Lambrea, D. M.; De Jeu, W. H. *Macromolecules* 2002, 35, 6930.
- Xu, J.-T.; Fairclough, J. P. A.; Mai, S.-M.; Ryan, A. J.; Chaibundit, C. *Macromolecules* 2002, 35, 6937.
- Muller, A. J.; Balsamo, V.; Arnal, M. L.; Jakob, T.; Schmalz, H.; Abetz, V. *Macromolecules* 2002, 35, 3048.

24. Lorenzo, A. T.; Arnal, M. L.; Muller, A. J.; Boschetti-De-Fierro, A.; Abetz, V. *Macromolecules* 2007, 40, 5023.
25. Castillo, R. V.; Muller, A. J.; Lin, M.-C.; Chen, H.-L.; Jeng, U.-S.; Hillmyer, M. A. *Macromolecules* 2008, 41, 6154.
26. Qiu, Z.; Yan, C.; Lu, J.; Yang, W. *Macromolecules* 2007, 40, 5047.
27. Li, Y.; Kaito, A.; Horiuchi, S. *Macromolecules* 2004, 37, 2119.
28. Kaito, A.; Li, Y.; Shimomura, M.; Nojima, S. *J Polym Sci Part B: Polym Phys* 2009, 47, 381.
29. He, Y.; Zhu, B.; Kai, W.; Inoue, Y. *Macromolecules* 2004, 37, 3337.
30. He, Y.; Zhu, B.; Kai, W.; Inoue, Y. *Macromolecules* 2004, 37, 8050.
31. Talibuddin, S.; Wu, L.; Runt, J.; Lin, J. S. *Macromolecules* 1996, 29, 7527.
32. Fillon, B.; Wittmann, J. C.; Lotz, B.; Thierry, A. *J Polym Sci Part B: Polym Phys* 1993, 31, 1383.
33. Feng, Y.; Jin, X. *J Appl Polym Sci* 1999, 72, 1559.
34. Balsamo, V.; Paolini, Y.; Muller, A. J. *Macromol Chem Phys* 2000, 201, 2711.
35. Wang, K.; Mai, K.; Han, Z.; Zeng, H. *J Appl Polym Sci* 2001, 81, 78.
36. Gu, Q.; Wu, L.; Wu, D.; Shen, D. *J Appl Polym Sci* 2001, 81, 498.
37. Lorenzo, A. T.; Arnal, M. L.; Sanchez, J. J.; Muller, A. J. *J Polym Sci Part B: Polym Phys* 2006, 44, 1738.
38. Avella, M.; Martuscelli, E.; Ramio, M. *Polymer* 1993, 34, 3234.
39. Barham, P. J. *J Mater Sci* 1984, 19, 3826.
40. Khasanova, A. K.; Wolf, B. A. *Macromolecules* 2003, 36, 6645.